

Bayesian recurrent state space model for rs-fMRI

Arunesh Mittal[†]
 Scott Linderman[§]
 John Paisley[†]
 Paul Sajda[†]

ARUNESH.MITTAL@COLUMBIA.EDU
 SCOTT.LINDERMAN@STANFORD.EDU
 JPAISLEY@COLUMBIA.EDU
 PSAJDA@COLUMBIA.EDU

[†]Columbia University, [§]Stanford University

Abstract

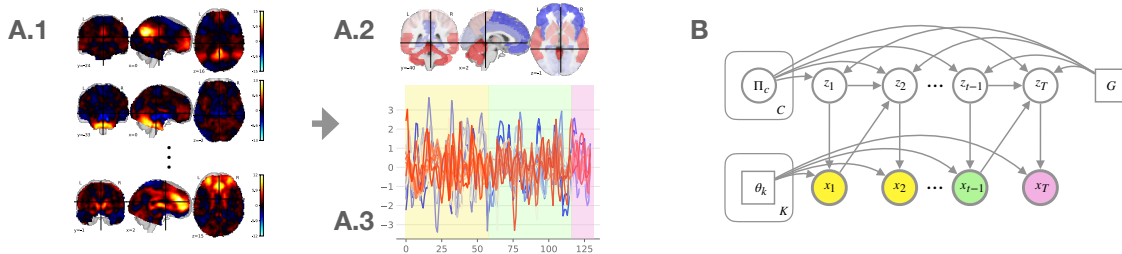
We propose a hierarchical Bayesian recurrent state space model for modeling switching network connectivity in resting state fMRI data. Our model allows us to uncover shared network patterns across disease conditions. We evaluate our method on the ADNI2 dataset by inferring latent state patterns corresponding to altered neural circuits in individuals with Mild Cognitive Impairment (MCI). In addition to states shared across healthy and individuals with MCI, we discover latent states that are predominantly observed in individuals with MCI. Our model outperforms current state of the art deep learning method on ADNI2 dataset.

1. Introduction

Resting state fMRI (rs-fMRI) measures the intrinsic spontaneous activity across brain regions, in the absence of any sensory or cognitive stimulus, and has proven to be a useful tool in understanding the functional architecture of the brain. The functional network patterns estimated from this spontaneous brain activity have prognostic, diagnostic, as well as interventional utility. Alterations in functional network patterns have been observed in neuropathologies such as Alzheimer’s, Depression, Schizophrenia, Autism and ADHD (Zhang and Raichle, 2010; Lee et al., 2013; Fox and Greicius,

2010). In contrast to task-based fMRI, rs-fMRI improves accessibility of these methods to a much wider patient population, as it can be used in patients with motor or cognitive deficits, language barriers, infants, and aging patient populations, unable to perform directed tasks. Vidaurre et al. (2017) showed that there are hierarchically organized stochastic recurring network patterns in rs-fMRI data in healthy subjects, which are both heritable and associated with specific cognitive traits. Several previous studies have applied standard state space models to rs-fMRI data (Suk et al., 2016; Zhang et al., 2019; Eavani et al., 2013; Ou et al., 2013; Wee et al., 2014; Liu et al., 2011), however, these models have two limitations: 1) They do not model the shared connectivity patterns across healthy and disease groups 2) They do not account for the recurrent state patterns observed by Vidaurre et al. (2017).

Building upon these prior works, we propose a state space model to uncover the spatio-temporal correlation patterns observed in rs-fMRI data. We model both class specific recurrent state transitions, as well as shared covariance structure across the classes. This allows modeling of the state switching behavior across different classes, as well as being able to delineate the network patterns shared across all classes, from the patterns dominant in only a particular class.



A) The rs-fMRI data for each individual (A.1) is aligned to a shared parcellation template (A.2) and the mean fMRI activity in each region is computed for all volumes in a sequence. This provides a lower dimensional temporal sequence $x_{1:T}$ for each individual (A.3). **B)** The probabilistic graphical model corresponding to the sequential generative process. The latent state sequence z_t given z_{t-1}, x_{t-1} for a class c is modeled using an activity dependent transition matrix $\Psi_c^{(t)} \triangleq f(\Pi_c, G, x_{t-1})$. Given a state $z_t = k$ at time t , the rs-fMRI ROI mean and inter-ROI covariance is modeled as $\mathcal{N}(\mu_k, \Sigma_k)$. The spatial ROI correlations are modeled by Σ_k , while the temporal recurrence is modeled by Ψ_c , together these two processes capture the space and time dynamics in the data.

2. Hierarchical recurrent state space model

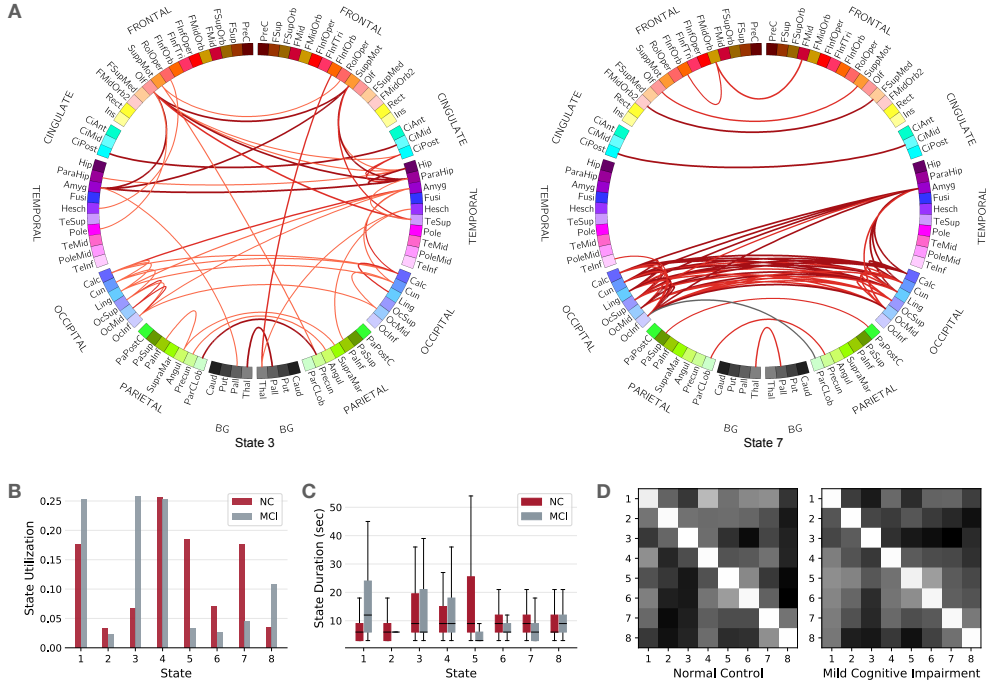
For a given sequence of fMRI activity $x_{1:T}$ across different regions of interest (ROI), we model the brain dynamics as a recurrent Markovian process where state $z_t \in \{1, \dots, K\}$ at time t depends on both the state at previous time step z_{t-1} , as well as the observations at the previous time step $x_{t-1} \in \mathbb{R}^D$ via a transition function $G : \mathbb{R}^D \rightarrow \mathbb{R}^K$. Given the latent state z_t at a time t , the mean μ_{z_t} and the covariance Σ_{z_t} , model the mean and the covariance across all ROIs. Since changes in the BOLD signal in fMRI vary relatively slowly due to the hemodynamic response time, we impose a weak “sticky” Dirichlet prior on the transition matrix to encourage slower state transitions.

To model class specific differences in the brain across health and pathologic classes, we propose class conditional transition matrices $\{\Pi_c\}_{c \in \{1, \dots, C\}}$. While the transition matrices are specific to each class, the observation parameters $\{\theta\}_{k=1}^K \triangleq \{\mu_k, \Sigma_k\}_{k=1}^K$ and transition function G , are shared across all classes.

The class conditional transition matrices together with the shared observation parameters, allow us to infer the dominant class as well as shared latent states across the two classes. Additionally, this parameter tying allows us to compare the discovered latent structure across all disease classes (Fig 2). This model structure encodes our belief that there are some states that are shared between the classes, and some states that are largely utilized by only one of the classes. The complete generative process is as follows:

$$\begin{aligned}
 y^{(n)} &\sim \text{Discrete}(p) \\
 [\Pi_{y^{(n)}}]_{k,:} &\sim \text{Dir}(\alpha \mathbf{1}_K + \kappa e_k) \\
 [\Psi_{y^{(n)}}]_{k,:}^{(t)} &\triangleq \frac{[\Pi_{y^{(n)}}]_{k,:} \odot \exp(Gx_{t-1})^\top}{\mathcal{Z}_k} \\
 z_t^{(n)} | z_{t-1}^{(n)} &\sim [\Psi_{y^{(n)}}]_{k,:}^{(t)} \\
 x_t^{(n)} &\sim \mathcal{N}(\mu_{z_t^{(n)}}, \Sigma_{z_t^{(n)}})
 \end{aligned}$$

where $[\Pi_c]_{k,:} \in \Delta_{K-1}$ is the k^{th} row of the $K \times K$ transition matrix Π_c for class c , \mathcal{Z}_k is normalizing constant for k^{th} row of the recurrent transition matrix and $G \in \mathbb{R}^{K \times D}$ is the recurrent state perturbation matrix (See Appendix B).



A) Uncovered covariance across ROIs, for most discriminative latent states, Σ_3 and Σ_7 , where for state k , a chord from region i to j corresponds to inter-ROI covariance $\Sigma_{k_{i,j}}$. The inner circle represents the anatomical regions for each ROI, the outer circle specifies the larger anatomical group the ROIs belongs to. **B)** Relative state utilization by Normal Control vs. MCI individuals. **C)** State durations for Normal Control vs. MCI individuals. **D)** Class conditional transition matrices for NC and MCI.

3. Inference

Our hierarchical model structure lends itself to a relatively simple modification of the standard message passing EM algorithm (Dempster et al., 1977) for HMMs (Rabiner, 1989). To maximize the joint likelihood of the data $p(x_{1:T}^{(n)}, z_{1:T}^{(n)} | \{\Pi_c\}_{c=1}^C, y^{(n)} | G, \{\theta\}_{k=1}^K)$, we first marginalize out the latent states $z_{1:T}^{(n)}$ for each class $y^{(n)} \in \{1, \dots, C\}$, and then proceed with the optimization M-step to update the shared parameters $\{\{\theta_k\}_{k=1}^K, G\}$ and the class specific parameters $\{\Pi_c\}_{c=1}^C$.

To marginalize the states in ①, for each class y , we only require the class conditional posterior marginals $q_c(z_t^{(n)}) \triangleq p(z_t^{(n)} | \{\theta\}_{k=1}^K, \Pi_c, x_{1:T}^{(n)})$. For ② we only re-

quire the class conditional two-slice marginal $q(z_t^{(n)}, z_{t-1}^{(n)}) \triangleq p(z_t^{(n)}, z_{t-1}^{(n)} | \{\theta\}_{k=1}^K, \Pi_c, x_{1:T}^{(n)})$. Hence, we can use the standard message passing algorithm to compute the class conditional posteriors for each class separately.

$$\begin{aligned}
 & \sum_{n,c} \log p(x_{1:T}^{(n)}, \Pi, y^{(n)} | G, \theta) = \\
 & \sum_{n,c} \underbrace{\mathbb{E}_{q_c(z)} \left[\log p(x_t^{(n)} | z_t^{(n)}, \theta) \mathbb{1}[y^{(n)}=c] \right]}_{\textcircled{1}} \\
 & + \underbrace{\mathbb{E}_{q_c(z)} \left[\log p(z_t^{(n)} | z_{t-1}^{(n)}, G, \Pi_c) \mathbb{1}[y^{(n)}=c] \right]}_{\textcircled{2}} \\
 & + \underbrace{\log p(\Pi_c)}_{\textcircled{3}}
 \end{aligned}$$

Table 1: Comparison with Deep-Autoencoder-HMM on ADNI2 dataset

Methods	Accuracy	Sensitivity	Specificity	Pos. Pred. Val.	Neg. Pred. Val.
Suk et al.	72.58	70.59	75	77.42	67.84
Ours	79.17	83.33	75	76.92	81.82

After marginalization, we then use gradient methods to update the parameters $\{\{\theta\}_{k=1}^K, G, \{\Pi_c\}_{c=1}^C\}$, to maximize the complete data log-likelihood $\sum_{n,c} \mathbb{E}_{q_c(z^{(n)})} [\log p(x_{1:T}^{(n)}, z_{1:T}^{(n)}, \Pi, y^{(n)} | G, \theta)]$ (See Appendix A and B for algorithm).

4. Experiments

We constructed our dataset by extracting all rs-fMRI images from the ADNI2 ¹ dataset. We matched the age and gender between the two groups: subjects diagnosed with Mild Cognitive Impairment (Mean age: 71.72 ± 2.82) and normal control subjects (Mean age: 71.65 ± 2.90). This resulted in a dataset of 116 subjects, with sequence length $T = 130$. Following the pre-processing steps used by Challis et al. (2015) (see: Fig. 1, Appendix D), each brain volume was parcellated into physiologically meaningful pre-defined regions of interest by warping and masking each subjects scan using the AAL atlas by Tzourio-Mazoyer et al. (2002). We then computed the mean time course for each region by computing the mean region of interest activity for each time point in a sequence. For training and test, we split up our dataset into age matched train ($N = 92$) and test set ($N = 24$). We chose hyper-parameters by 5-fold cross-validation on the train dataset. For the presented results we used $\{K = 8, \alpha = .5, \kappa = 100\}$. We report results on the heldout set in Table 1, where we predict the disease class using the Bayes classifier with

uniform prior probability over classes: $\hat{y} = \arg \max_y \mathbb{E}_{q_y(z^{(n)})} [\log p(x^{(n)}, z^{(n)}, \Pi, y | G, \theta)]$.

5. Conclusion

Our method allows us to model temporal recurrent dynamics, which are influenced by class specific local parameters $\{\Pi_c\}_{c=1}^C$ and class agnostic global parameter G . The hierarchical structure then lets us compare the network patterns associated with each of the disease classes. We compare the uncovered correlations associated with the most prevalent states in MCI and NC individuals. We observe stronger inter-hemispheric cortical connections in healthy individuals. In addition, we observe stronger inter-hemispheric connectivity across occipital regions in healthy subjects. These findings have been independently reported by previous voxel-mirrored homotopic connectivity analysis in individuals with MCI (Wang et al., 2015). In future work, we plan to evaluate our method on additional rs-fMRI datasets for other neuropathologies. To improve the model capacity, we will explore a more flexible non-linear likelihood model. Lastly, given the high dimensionality of the voxel data, we also plan to investigate incorporating additional prior structure on the covariance matrices, reflective of the anatomical connectivity constraints. In addition to the phenotype matching approach proposed in this work, we hope to extend this approach to uncover latent phenotypes (Chen et al., 2020) from rs-fMRI data.

¹<http://adni.loni.usc.edu/>

References

- Edward Challis, Peter Hurley, Laura Serra, Marco Bozzali, Seb Oliver, and Mara Cercignani. Gaussian process classification of alzheimer’s disease and mild cognitive impairment from resting-state fmri. *NeuroImage*, 112:232–243, 2015.
- Irene Y Chen, Shalmali Joshi, Marzyeh Ghassemi, and Rajesh Ranganath. Probabilistic machine learning for healthcare. *arXiv preprint arXiv:2009.11087*, 2020.
- Arthur P Dempster, Nan M Laird, and Donald B Rubin. Maximum likelihood from incomplete data via the em algorithm. *Journal of the Royal Statistical Society: Series B (Methodological)*, 39(1):1–22, 1977.
- Harini Eavani, Theodore D Satterthwaite, Raquel E Gur, Ruben C Gur, and Christos Davatzikos. Unsupervised learning of functional network dynamics in resting state fmri. In *International conference on information processing in medical imaging*, pages 426–437. Springer, 2013.
- Michael D Fox and Michael Greicius. Clinical applications of resting state functional connectivity. *Frontiers in systems neuroscience*, 4:19, 2010.
- Megan H Lee, Christopher D Smyser, and Joshua S Shimony. Resting-state fmri: a review of methods and clinical applications. *American Journal of neuroradiology*, 34(10):1866–1872, 2013.
- Wei Liu, Suyash P Awate, Jeffrey S Anderson, Deborah Yurgelun-Todd, and P Thomas Fletcher. Monte carlo expectation maximization with hidden markov models to detect functional networks in resting-state fmri. In *International Workshop on Machine Learning in Medical Imaging*, pages 59–66. Springer, 2011.
- Jinli Ou, Li Xie, Peng Wang, Xiang Li, Dajiang Zhu, Rongxin Jiang, Yufeng Wang, Yaowu Chen, Jing Zhang, and Tianming Liu. Modeling brain functional dynamics via hidden markov models. In *2013 6th International IEEE/EMBS Conference on Neural Engineering (NER)*, pages 569–572. IEEE, 2013.
- Lawrence R Rabiner. A tutorial on hidden markov models and selected applications in speech recognition. *Proceedings of the IEEE*, 77(2):257–286, 1989.
- Heung-Il Suk, Chong-Yaw Wee, Seong-Whan Lee, and Dinggang Shen. State-space model with deep learning for functional dynamics estimation in resting-state fmri. *NeuroImage*, 129:292–307, 2016.
- Nathalie Tzourio-Mazoyer, Brigitte Landeau, Dimitri Papathanassiou, Fabrice Crivello, Olivier Etard, Nicolas Delcroix, Bernard Mazoyer, and Marc Joliot. Automated anatomical labeling of activations in spm using a macroscopic anatomical parcellation of the mni mri single-subject brain. *Neuroimage*, 15(1):273–289, 2002.
- Diego Vidaurre, Stephen M Smith, and Mark W Woolrich. Brain network dynamics are hierarchically organized in time. *Proceedings of the National Academy of Sciences*, 114(48):12827–12832, 2017.
- Zhiqun Wang, Jianli Wang, Han Zhang, Robert Mchugh, Xiaoyu Sun, Kuncheng Li, and Qing X Yang. Interhemispheric functional and structural disconnection in alzheimer’s disease: a combined resting-state fmri and dti study. *PLoS One*, 10(5):e0126310, 2015.
- Chong-Yaw Wee, Pew-Thian Yap, Daoqiang Zhang, Lihong Wang, and Dinggang Shen. Group-constrained sparse fmri connectivity modeling for mild cognitive impairment

- identification. *Brain Structure and Function*, 219(2):641–656, 2014.
- Dongyang Zhang and Marcus E Raichle. Disease and the brain’s dark energy. *Nature Reviews Neurology*, 6(1):15–28, 2010.
- Gemeng Zhang, Biao Cai, Aiyong Zhang, Julia M Stephen, Tony W Wilson, Vince D Calhoun, and Yu-Ping Wang. Estimating dynamic functional brain connectivity with a sparse hidden markov model. *IEEE transactions on medical imaging*, 39(2):488–498, 2019.

Appendix A. Full EM algorithm

Algorithm 1 EM for hierarchical recurrent state space model

Initialize $\{\theta_k\}_{k=1}^K \triangleq \{\mu_k, \Sigma_k\}_{k=1}^K$ ▷ Initialize with empirical Bayes GMM

Random Initialization $\{\{\Pi_c\}_{c \in \{1, \dots, C\}}, G\}$

```

for  $m \in \{1, \dots, M\}$  do
  ▷ M iterations
  for  $n \in \{1, \dots, N\}$  do
    ▷ N ROI sequences
    for  $c \in \{1, \dots, C\}$  do
      ▷ Forwards Backwards for each class
       $\{q_c(z_t^{(n)}), q_c(z_t^{(n)}, z_{t-1}^{(n)})\} \leftarrow \text{ForwardsBackwards}(x_{1:T}^{(n)}, \{\theta_k\}_{k=1}^K, \Pi_c)$ 
    end
  end

  for  $k \in \{1, \dots, K\}$  do
    ▷ Analytic update state parameters
     $\{\mu_k, \Sigma_k\} \leftarrow \operatorname{argmax}_{\{\mu_k, \Sigma_k\}} \sum_y \sum_n \mathbb{E}_{q_c(z_{1:T}^{(n)})} \left[ \mathbf{1}[y^{(n)} = c] \log p(x_t^{(n)} | z_t^{(n)}, \{\theta_k\}_{k=1}^K) \right]$ 
  end

  for  $l \in \{1, \dots, L\}$  do
    ▷ L iterations
    ▷ M-step for transition function
     $\tilde{G} \leftarrow \tilde{G} + \eta \nabla_{\tilde{G}} \sum_y \mathbb{E}_{q_c(z_{1:T}^{(n)})} \left[ \log p(z_t^{(n)} | z_{t-1}^{(n)}, e^{(\tilde{G})}, \Pi_c) \right]$ 

    for  $c \in \{1, \dots, C\}$  do
      ▷ M-step for transition matrices
       $\tilde{\Pi}_c \leftarrow \tilde{\Pi}_c + \eta \nabla_{\tilde{\Pi}_c} \sum_c \left( \mathbf{1}[y^{(n)} = c] \mathbb{E}_{q_c(z_{1:T}^{(y)})} \left[ \log p(z_t^{(y)} | z_{t-1}^{(y)}, \log(\tilde{G}), e^{(\tilde{\Pi}_c)}) \right] + \log p(e^{(\tilde{\Pi}_c)}) \right)$ 
    end
  end
end

```

Appendix B. Generative Model

B.1. Hierarchical recurrent Markov model

$$\prod_n p\left(x_{1:T}^{(n)}, y^{(n)}, \{\Pi_c\}_{c=1}^C | G, \{\theta_k\}_{k=1}^K\right) \quad (1)$$

$$= \prod_c \prod_n \prod_t \left(p(x_t^{(n)} | z_t^{(n)}, \{\theta_k\}_{k=1}^K) p(z_t^{(n)} | z_{t-1}^{(n)}, G, x_{t-1}^{(n)}, \Pi_c) p(\Pi_c) p(y^{(n)}) \right)^{\mathbb{1}[y^{(n)}=c]} \quad (2)$$

$$= \prod_c \prod_n \prod_t \prod_{i,j} p(x_t^{(n)} | \theta_{z_t^{(n)}}) \mathbb{1}[z_t^{(n)}=i] \quad (3)$$

$$\left(p(z_t^{(n)} | z_{t-1}^{(n)}, G, x_{t-1}^{(n)}, \Pi_c) \mathbb{1}[z_t^{(n)}=i, z_{t-1}^{(n)}=j] p(\Pi_c) p(y^{(n)}) \right)^{\mathbb{1}[y^{(n)}=c]} \quad (4)$$

B.2. Recurrent transition model with sticky transition prior

$$p(z_t^{(n)} | z_{t-1}^{(n)} = k, G, x_{t-1}^{(n)}, \Pi_c) p(\Pi_c) \quad (5)$$

$$= \text{Discrete} \left(z_t^{(n)} \mid \frac{[\Pi_c]_{k,:} \odot \exp(Gx_{t-1})^\top}{\mathcal{Z}_k} \right) \text{Dir}([\Pi_c]_{k,:} | \alpha \mathbf{1}_K + \kappa e_k) \quad (6)$$

Where \mathcal{Z}_k is normalizing constant for k^{th} row of the recurrent transition matrix and $G \in \mathbb{R}^{K \times D}$ is the recurrent state perturbation matrix.

Appendix C. Inference

C.1. Expected complete data log-likelihood

$$\begin{aligned} & \sum_n \log p(x_{1:T}^{(n)}, \{\Pi_c\}_{c=1}^C | \{\theta_k\}_{k=1}^K, G) \\ &= \sum_n \mathbb{E}_{q(z^{(n)})} \left[\log p(x_{1:T}^{(n)}, \{\Pi_c\}_{c=1}^C | \{\theta_k\}_{k=1}^K, G) \right] \end{aligned} \quad (7)$$

$$= \sum_c \sum_{\{n: y^{(n)}=c\}} \sum_t \sum_i \left(q_c(z_t^{(n)} = i) \log p(x_t^{(n)} | \theta_{z_t^{(n)}}) + \quad (8)$$

$$\sum_j q_c(z_t^{(n)} = i, z_{t-1}^{(n)} = j) \log p(z_t^{(n)} | z_{t-1}^{(n)}, G, x_{t-1}^{(n)}, \Pi_c) + \log p(\Pi_c) \right) \quad (9)$$

Where class conditional posterior $q_c(z_t^{(n)})$ and $q_c(z_t^{(n)}, z_{t-1}^{(n)})$ can be computed using the standard Baum-Welch algorithm.

C.2. Gradient update for Π_c

$$\Pi_c \triangleq \exp(\tilde{\Pi}_c)$$

$$\begin{aligned} \nabla_{\tilde{\Pi}_c} \sum_n \log p(x_{1:T}^{(n)}; \{\theta_k\}_{k=1}^K, G, \tilde{\Pi}_c) \\ = \sum_{\{n:y^{(n)}=c\}} \sum_t \sum_{i,j} \nabla_{\tilde{\Pi}_c} q_c(z_t^{(n)} = i, z_{t-1}^{(n)} = j) \log p(z_t^{(n)} | z_{t-1}^{(n)}, G, x_{t-1}^{(n)}, \tilde{\Pi}_c) \end{aligned} \quad (10)$$

$$\Pi_c \leftarrow \exp \left(\tilde{\Pi}_c + \rho \sum_{\{n:y^{(n)}=c\}} \sum_t \sum_{i,j} \nabla_{\tilde{\Pi}_c} q_c(z_t^{(n)} = i, z_{t-1}^{(n)} = j) \log p(z_t^{(n)} | z_{t-1}^{(n)}, G, x_{t-1}^{(n)}, \tilde{\Pi}_c) \right) \quad (11)$$

Appendix D. Preprocessing

We smoothed the 3D volumes with a 8 mm^3 FWHM 3D Gaussian kernel, followed by filtering the data with a band-pass filter (0.01 to 0.08 Hz). We discarded the first 10 volumes of each sequence to avoid saturation effects. Each brain volume was parcellated into physiologically meaningful pre-defined regions of interest by warping and masking each subjects scan using the AAL atlas by [Tzourio-Mazoyer et al. \(2002\)](#). To reduce the dimensionality of the data, we discard atlas regions (90 - 116 inclusive), corresponding to the Cerebellum.